

3D Printed Stem-Cell-Laden, Microchanneled Hydrogel Patch for the Enhanced Release of Cell-Secreting Factors and Treatment of Myocardial Infarctions

Molly R. Melhem,[†] Jooyeon Park,[‡] Luke Knapp,[§] Larissa Reinkensmeyer,[§] Caroline Cvetkovic,[†] Jordan Flewellyn,[§] Min Kyung Lee,[‡] Tor Wolf Jensen,[⊥] Rashid Bashir,^{†,||} Hyunjoon Kong,^{*,‡,†,||} and Lawrence B. Schook^{§,†,||}

[†]Department of Bioengineering, University of Illinois at Urbana–Champaign, 1270 Digital Computer Laboratory, MC-278, Urbana, Illinois 61801-2987, United States

[‡]University of Illinois at Urbana–Champaign, Department of Chemical and Biomolecular Engineering 114 Roger Adams Laboratory, MC 712, 600 South Mathews Avenue, Urbana, Illinois 61801-3602, United States

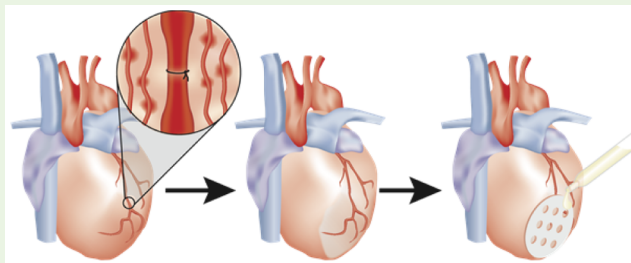
[§]Department of Animal Sciences, University of Illinois at Urbana–Champaign, 1207 West Gregory Drive, Urbana, Illinois 61801-4733, United States

[⊥]Division of Biomedical Sciences, University of Illinois at Urbana–Champaign, Urbana, Illinois 61801, United States

^{||}Carl R. Woese Institute for Genomic Biology, University of Illinois at Urbana–Champaign, 1206 West Gregory Drive, MC-195, Urbana, Illinois 61801, United States

ABSTRACT: Over the past several years, biomaterials loaded with mesenchymal stem cells (MSCs) have increasingly been used to reduce the myocardial fate of postinfarction collagen deposition and scar tissue formation. Despite successful gains, therapeutic efficacy has remained limited because of restricted transport of cell-secreting factors at the site of implantation. We hypothesized that an MSC-laden hydrogel patch with multiple microchannels would retain transplanted cells on target tissue and support transport of cell-secreting factors into tissue. By doing so, the gel patch will improve the therapeutic potential of the cells and minimize the degradation of myocardial tissue postinfarction. To examine this hypothesis, a stereolithographic apparatus (SLA) was used to introduce microchannels of controlled diameters (e.g., 500 and 1000 μm) during in situ cross-linking reaction of poly(ethylene glycol)dimethacrylate solution suspended with cells. Placement of the MSC-laden, microchanneled gel patch on the occluded left coronary artery in a murine model showed significant improvement in the ejection fraction, fractional shortening, and stroke volume, compared with gel patches without MSCs and MSC-laden gel patches without microchannels. In particular, the microchannels significantly reduced the number of cells required to recover cardiac function, while minimizing cardiac remodeling. In sum, the microchanneled gel patch would provide a means to prevent abnormal fibrosis resulting from acute ischemic injury.

KEYWORDS: hydrogel, biotransport, stereolithographic apparatus, mesenchymal stem cells, fibrosis, cardiac remodeling, ischemia



INTRODUCTION

Despite medical progress in treatment and intervention, atherosclerotic cardiovascular disease is still a leading cause of morbidity and mortality worldwide. Current techniques to treat infarction involve removing vascular plaques and restoring blood flow to the injured cardiac muscle, potentially decreasing the permanent tissue damage resulting from hypoxia.^{1–4} This approach, while beneficial, often stimulates an undesirable burst of reactive oxygen species, termed ischemia-reperfusion injury, that inadvertently increases the severity of tissue damage.^{5,6} Therefore, it is crucial to develop a therapeutic method that can prevent the destructive myocardium remodeling and subsequent fatal heart failure.

Mesenchymal stem cells (MSCs) that can be derived from a patient's own bone marrow or adipose tissue have been studied as a new generation of medicine to treat myocardial infarction.^{7–10} MSCs can sustainably produce and release therapeutic molecules that control apoptosis, inflammatory response, and revascularization in damaged tissue.^{11,12} The secretion activities of MSCs can be further stimulated with

Special Issue: Tissue Engineering

Received: March 31, 2016

Accepted: July 5, 2016

proper soluble and insoluble signals, increasing their therapeutic potential.^{13–15}

A variety of strategies have been employed to deliver MSCs to infarcted tissue and control molecular secretion activities: (1) direct intramyocardial injection of cells to the injured site; (2) systemic intravenous infusion; and (3) local coronary delivery via a catheter placed within the coronary vessels. All three of these means have demonstrated an initial decrease in infarct size, ventricular remodeling, and improved vascularization.^{10,16–18} Although these reports are encouraging, it has been reported that 7 days after transplantation, stem cell concentration at the site of injection decreases by 10-fold, with no trace of stem cells after 3 weeks, resulting in limited therapeutic efficacy of cells over a desired treatment period.^{17,19} Consequently, the repeated cell transplantation on a regulated or on-demand basis is required for cardiac repair, an approach that can be plagued by limited cell source and massive medical costs.

One proposed solution that has emerged to resolve this challenge is to implant an MSC-loaded gel patch to damaged cardiac tissue. The patch can be designed to maintain structural stability under physiologically relevant deformation and minimize the displacement of cells compared with cells injected into cardiac muscle or delivered to coronary arteries.^{20–23} The rigidity and permeability of gels can be tailored to support cellular viability and secretion activities, specifically when gels are suspended in cell culture media.^{24–29} However, for a gel implanted on tissue, interface between the gel patch and tissue often acts as a barrier to limit the release of cell-secreting factors.

To this end, we hypothesized that loading MSCs into a hydrogel assembled to present microchannels of controlled diameters using a three-dimensional (3D) printer would facilitate the release of paracrine factors on the implanted tissue. The resulting MSC-loaded gel patch would be useful in retaining cardiac function of the damaged heart due to ischemia. To examine this hypothesis, we loaded bone marrow-derived MSCs (BMSCs) into a hydrogel patch by cross-linking poly(ethylene glycol) dimethacrylate (PEGDMA) solution suspended with cells. The microchannels with a desired diameter were incorporated into the cell-loaded hydrogel via in situ cross-linking reaction using a stereolithographic assembly (SLA) unit.³⁰ By doing so, the microchannels serve as a drainage of cell-secreted growth factors to tissue.³¹ MSCs immobilized within the gels without microchannels were also used as a control. The resulting cell-gel construct was implanted on cardiac muscle that was damaged by clamping the main coronary artery.³¹ Therapeutic efficacy of the implant was assessed by measuring cardiac contraction using echocardiography, and the degree of cardiac fibrosis using histology.

MATERIALS AND METHODS

Cell Culture. Human bone marrow-derived MSCs (Lonza, Basel, Switzerland) were cultured in TheraPEAK MSCGM-CD mesenchymal stem cell medium (Lonza) supplemented with 5% fetal bovine serum (FBS, Gibco, Carlsbad, CA, USA), 100 U mL⁻¹ penicillin, and 100 mg mL⁻¹ streptomycin (Gibco). Cells were incubated at 37 °C and 5% O₂ in 175 cm² flasks to 80% confluence. When preparing for cell-encapsulation, cells were lifted with 0.25% trypsin and 0.04% EDTA in HBSS (Gibco) and gently added to the pregel solution.

Microvascular Stamp: 3D Printing of Microchanneled, MSC-Laden Hydrogel. The microvascular stamp fabrication method was described in detail in a previous publication.³⁰ In brief, poly(ethylene glycol) dimethacrylate (PEGDMA) with a molecular weight of 1000

Da (Sigma-Aldrich, St. Louis, MO, USA) was dissolved in sterile phosphate buffer saline (PBS) to prepare a 20% w/v solution prepolymer solution. The photoinitiator, 1-[4-(2-hydroxy-ethoxy)-phenyl]-2-hydroxy-2-methyl-1-propane-1-one (Irgacure 2959, Ciba, Tarrytown, NY, USA), was dissolved in DMSO and added to the pregel solution for a final concentration of 0.5% w/v. Depending on the desired condition, medium either with or without cells was mixed with the pregel PEGDMA solution immediately before fabrication. The cell density in the solution was varied from 0 to 0.4 × 10⁶ and 2.0 × 10⁶ cells/mL. A precise amount of prepolymer solution sterilized via filtration was transferred into a sterile apparatus designed to avoid the contamination of final gel constructs by the environment. All pregel solution preparations and gel assembly were done under a laminar flow hood. A stereolithography apparatus (SLA, Model 250/50, 3D Systems, Rock Hill, SC, USA) was used to fabricate the cell-encapsulating hydrogel constructs with controlled spatial organization of microchannels. Computer aided design models were generated using AutoCAD 2009 (Autodesk, San Rafael, CA, USA) and exported to stereolithography (STL) format. The SLA software, 3D Lightyear v1.4 (3D Systems, Rock Hill, SC, USA) was used to slice the 3D models into a series of 2D layers from a user-specified thickness. A laser power of about 15 mW and an average energy dose of 1600 mJ cm⁻² was used to assemble the gel constructs via in situ photo polymerization. The laser intensity and dose were optimized in a previously published study.³⁰ Once the fabrication procedure was finished, the hydrogels were rinsed multiple times with 2 mL of culture media at each rinse to remove excess polymer and incubated using conventional sterile cell culture techniques.

Hydrogel Characterization. To assess for the role environmental factors played on the patch properties of elastic modulus and swelling ratio, we incubated the sterile constructs in media with a pH of 5.0 and 7.0 at 37 °C for 24 h following fabrication. For measurement of the elastic modulus (*E*), the constructs were subjected to a mechanical compression by an electromechanical tester (Insight, MTS Systems, Eden Prairie, MN, USA) at a constant deformation rate of 1.0 mm s⁻¹ at 25 °C. The elastic modulus was calculated using the slope of the stress (σ) vs strain (λ) curve. The swelling ratios of the gels were determined by measuring the weight of the swollen gels and the weight of the dried gels. The volumetric swelling ratio (*Q*) was calculated using the following equation

$$Q = \frac{(m_s - m_d) \frac{\rho_p}{\rho_w} + m_d}{m_d} \quad (1)$$

Where m_s represents the mass of the swelled gel, m_d represents the mass of the dried gel, ρ_p is the density of the polymer, 20% w/v in our constructs, and ρ_w represents the density of water.

Cell Viability Tests. The 3D fabricated hydrogel processed in a form of 5 mm diameter and 0.2 mm thickness was transferred to a 96-well plate and incubated in 200 μ L of cell culture media until viability testing was completed. A live/dead viability/cytotoxicity test was performed using a kit (Life Technologies, Carlsbad, CA, USA). Briefly speaking, a working solution consisting of 1 μ L of calcein AM and 2 μ L of Ethidium homodimer-1 was added to 1 mL of sterile 1× PBS immediately prior to performing the assay. The media was removed from each construct-containing well and 150 μ L of the working solution was added. After 20 min, the cell-laden hydrogel disks were visualized with fluorescent microscope (Zeiss, LSM700).

Cellular Tropic Factor Secretion Assessment. The cell culture media used for BMSC culture was used to characterize the trophic factors secreted by cells. A human angiogenesis antibody array kit (R&D systems, Minneapolis, MN, USA) was used to analyze the cell culture media following the manufactures protocols. Briefly, culture media was diluted with a cocktail of prepared detection antibodies. The solution was then incubated overnight with a provided antibody spotted membrane. The membrane was then washed and developed using chemiluminescence, displaying an array of captured antibodies whose signal is proportionate to the amount of bound protein.

In parallel, the amount of VEGF in the cell culture media were quantified using a VEGF human ELISA kit (Life Technologies,

Carlsbad, CA, USA). Media was collected from cell encapsulating hydrogel constructs at days 1, 3, 5, and 7, and stored in $-20\text{ }^{\circ}\text{C}$. The media were thawed just prior to running the angiogenesis membrane assay. Collected media were incubated on a well plate containing VEGF antibodies fixed to its surface. After brief washes, an enzyme-linked detection antibody was added to the well plates to bind the VEGF antigen. Finally, a substrate designed to react with the linked enzyme was added to the plate. The absorbance of resulting color at 450 nm was recorded using a plate reader (Synergy HT, Biotek).

In Vivo Evaluation of Cell-Hydrogel Constructs Using a Myocardial Infarction Model. Prior to surgery, mice were anesthetized in an anesthetic chamber with 5% isoflurane accompanied by and 1 L/min supportive O_2 flow. Their weight was recorded and mice were intubated with a 20G angiocath tube and connected to a small animal ventilator (160 bpm), where 1.5% isoflurane and 1 L/min O_2 were administered. The mice were placed on a heating pad in the supine position. Hair was removed from the surgical site and an inch long vertical incision was made slightly to the left of center. Two muscle layers were teased back and sutured in the retracted position. An intercostal incision was made between the third and fourth ribs and the heart was exposed. A single 8–0 monofilament suture (Johnson & Johnson, NJ) was placed in the left coronary artery to occlude blood flow to the apex of the heart. The constructs were transferred to the myocardium with a bead-sterilized spatula directly following vessel occlusion. Using a 6–0 monofilament suture (Johnson & Johnson, NJ), the ribs and muscle layers were closed by interrupted suture and the skin layer incision was closed by continuous suture. The isoflurane administration was ceased before the removal of the tracheal tube from the mouse, and animals were monitored until full recovery.

Echocardiography. A VisualSonics Vevo 2100 (VisualSonics, Toronto, Canada) small animal ultrasound was used to perform echocardiography on the mice at 4wks postoperation. Animals were placed in an anesthetic chamber and 5% isoflurane was administered with 2 L/min of supportive O_2 . Once properly anesthetized, the animals were moved to a nose cone and the percent of isoflurane was decreased to 1.5–2%. The imaging area was cleared using a depilatory cream and 2D M-mode echocardiography was performed on the animals. All heart function calculations were made using the Vevo 2100 software.

Histological Analysis of Heart Sections. Animals were sacrificed at 4 and 8 weeks postoperation and their hearts were collected, fixed in a 10% formalin solution, and embedded in paraffin. Tissue was sliced and cross sections were stained for Hematoxylin and Eosin and Trichrome Blue. Digital images of the stained sections were collected with a NanoZoomer Slider Scanner/Digital Pathology System (Hamamatsu, Hamamatsu, SZK).

RESULTS

3D Printing of MSC-Laden Hydrogel Patch. The MSC-laden, microchanneled hydrogel patch was constructed by activating a cross-linking reaction of PEGDMA solution mixed with cell suspension using a stereolithography apparatus (SLA). The computer-controlled SLA unit, prescribed by a computer aided design (CAD) file, focused laser light directly on desired sites of the PEGDMA solution mixed with MSCs. This process enabled cross-linking at the site of light focus (Figure 1a). The laser-activated photo cross-linking reaction allowed detailed control of the three-dimensional features of the construct.

Previous work has demonstrated controlled and directed neovascularization through the incorporation of microchannel diameters less than $800\text{ }\mu\text{m}$, with diminished vascularization at larger diameters.³² To demonstrate this vascularization discrepancy, we introduced 9 separate microchannels, with diameters kept constant at 500 or $1000\text{ }\mu\text{m}$, in the MSC-laden gel patch using the SLA unit. An additional control patch without microchannels also prepared (Figure 1b). The resulting gel entrapped the cells in a hydrogel construct, thus minimizing

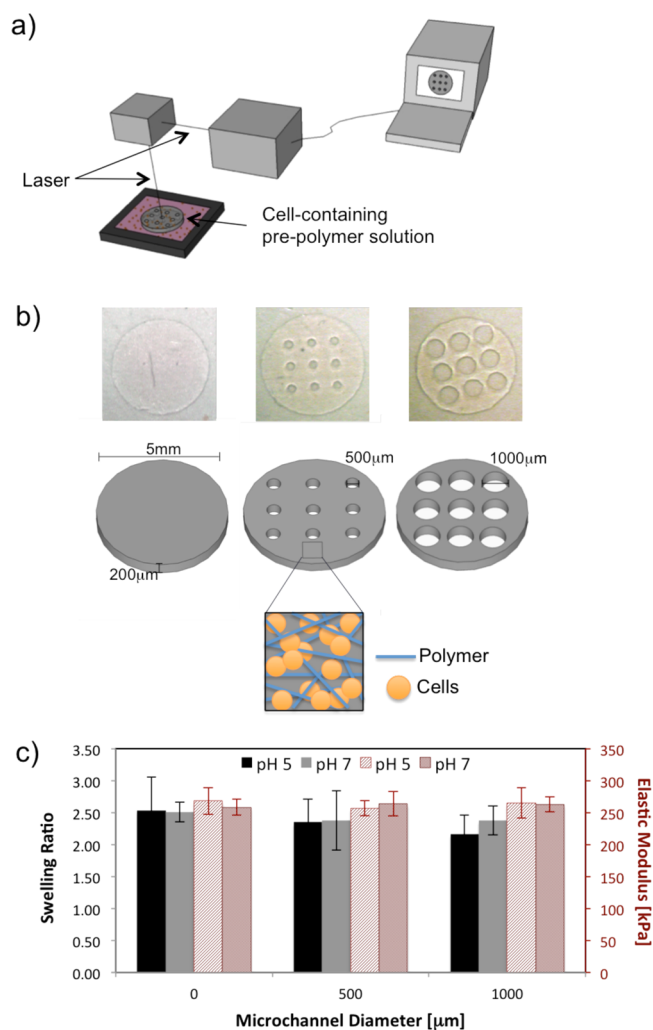


Figure 1. 3D printing of the MSC-laden gel patches with microchannels of controlled diameters. (a) Schematic representation of the stereolithography apparatus (SLA) process. A 3D CAD was developed and converted into the stereolithography format. The SLA then focused a UV light source on a cell-containing prepolymer solution. The focusing of the light resulted in cross-linking and subsequent encapsulation of the cells in the predefined design. (b) Three designs were chosen, one without microchannels, and two with 9 evenly spaced microchannels. The microchannel diameter was kept constant at 500 and $1000\text{ }\mu\text{m}$. (c) Neither the microchannel diameter nor the environmental conditions altered the swelling ratio and elastic moduli of the constructs.

cell displacement. The concentration of cells loaded in the gel was controlled to be 0, 0.4×10^6 , or 2.0×10^6 cells/mL, by altering the number of cells mixed with PEGDMA prepolymer solution. The incorporation of $500\text{ }\mu\text{m}$ -diameter microchannels slightly reduced the total number of cells loaded in the gel patch. In contrast, incorporation of $1000\text{ }\mu\text{m}$ -diameter microchannels led to 1.6-fold decrease in the number of cells laden in the gel.

Stability of Swelling and Mechanical Properties of the Constructs. The swelling ratio (Q) and elastic modulus (E) of each of the gel construct designs were measured (Figure 1c). At physiological conditions of pH of 7.0 and temperature of $37\text{ }^{\circ}\text{C}$, the incorporation of microchannels did not change the construct properties. To assess for the stability of the constructs under varied pH conditions, we incubated gel constructs in

media at pH of 5.0. The degree of swelling and the elastic moduli of the gel constructs were found to have statistically insignificant differences in differing environmental pH's.

Analysis of Cellular Survival and Cytokine Secretion Activities. To obtain a macroscopic view of the cell population and its changes over time, we performed a qualitative analysis of live/dead cell staining at day 1, 7, and 14. No significant difference in the number of viable cells between conditions was observed (Figure 2). In addition, independent of the micro-

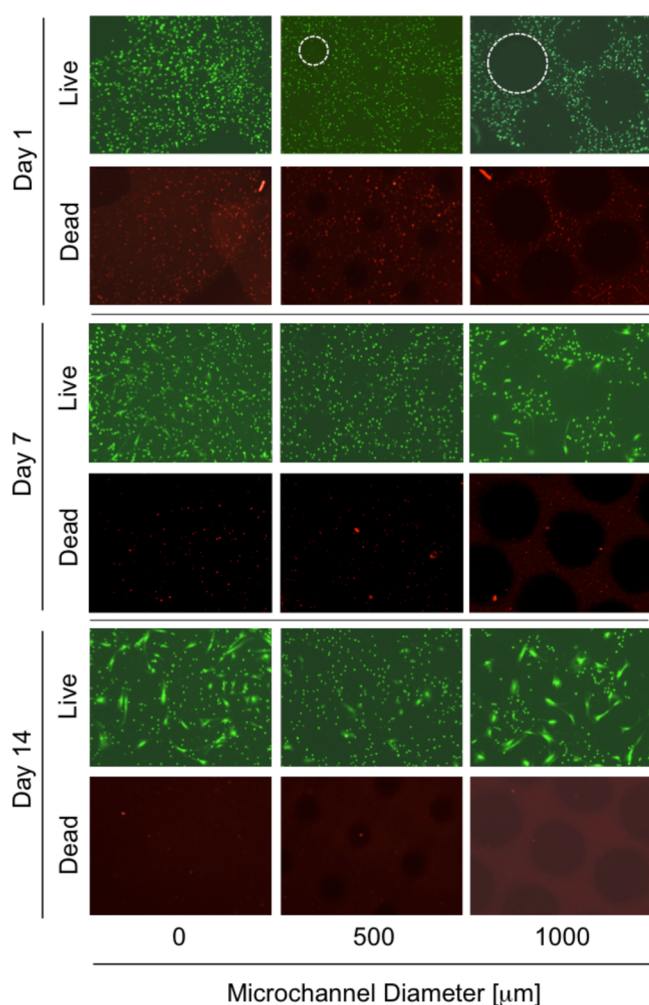


Figure 2. Live/dead analysis of MSCs laden in the gel using the pair of calcein (green, live cell marker)/ethidium homodimer (red, apoptotic, or necrotic cell marker). Dashed circles in the first row of images represent microchannels introduced into the gel patches. Cell density was kept constant at 2.0×10^6 cells/mL.

channel diameter, the number of viable cells stained by the hydrolyzed calcein was increased over 14 days of cell culture. Note that the calcein is hydrolyzed to fluorescent molecules on the live cell membrane. In parallel, few dead cells stained by the ethidium homodimer-1 were found for all conditions.

Next, the secretion profile of the encapsulated MSCs was examined by using the angiogenesis membrane assay kit. Cells cultured on a cell culture substrate release a series of proangiogenic factors [e.g., interleukin-8 (IL-8), vascular endothelial growth factor (VEGF)] and antiangiogenic factors [pigment epithelium-derived factor (PEDF)] (Figure 3a). Cells also secrete cytokines including tissue inhibitor of metal-

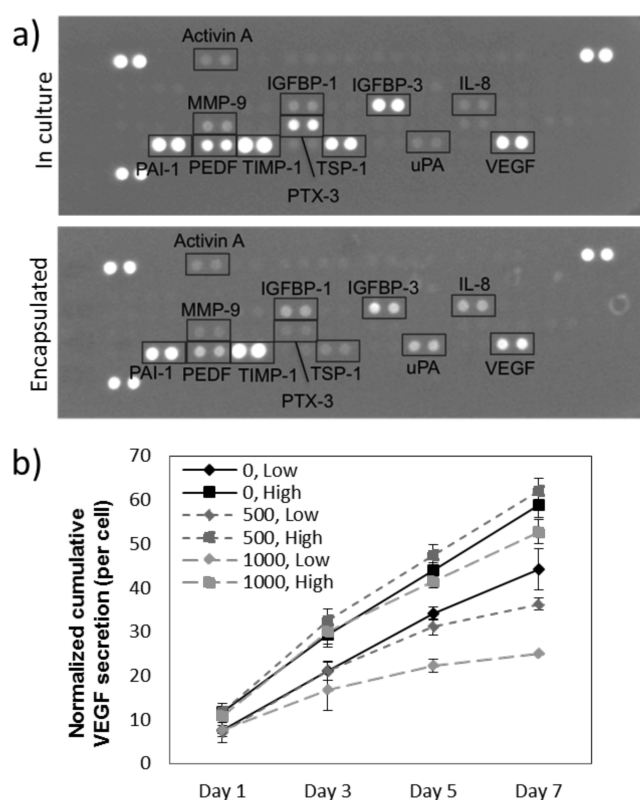


Figure 3. Analysis of secretion activities of MSCs. (a) An angiogenesis antibody array used to evaluate the relative levels of cytokines secreted from MSCs cultured on a plastic cell culture well and those encapsulated in a hydrogel with 500 μm diameter microchannels. The angiogenesis antibody array presents 55 angiogenesis-related proteins involved in proangiogenesis, antiangiogenesis, fibrosis, antiapoptosis, and tissue remodeling. (b) Normalized cumulative VEGF amount in the cell culture media incubated with MSC-laden gel patches. The cell density was kept constant at 0.4×10^6 cells/mL (marked with "low") and 2.0×10^6 cells/mL (marked with "high"). "0" represents the cell-free, blank gel patch. The cumulative VEGF amount was normalized to the initial number of cells loaded into the gel.

loproteinase-1 (TIMP-1), which decreases left ventricular remodeling, plasminogen activator inhibitor (PAI-1), which decreases cardiac fibrosis after myocardial infarction (MI). Additionally, cells release thrombospondin-1 (TSP-1) and pentraxin-related protein (PTX-3), both of which are known antiapoptotic cytokines.

Interestingly, MSCs encapsulated in gels reduced the expression levels of PEDF, PTX-3, and TSP-1, but kept the secretion activities of VEGF, PAI-1, and TIMP-1. These results suggest MSCs loaded in the gel patch can orchestrate a variety of pathways beneficial to prevent deterioration of heart remodeling following acute cardiac infarction and further treat the damaged muscle by stimulating neovascularization.

We further examined whether the cells can sustainably release cytokines by examining cellular release profile of VEGF over 2 weeks. As expected, the cumulative amount of VEGF released from cells into cell culture media was linearly increased over a week, independent of the diameter of microchannels (Figure 3b). According to the cumulative VEGF amount normalized to the number of encapsulated cells, increasing the encapsulated cell density significantly elevated the normalized cumulative VEGF concentration. In contrast, the microchannel diameter made insignificant influence on the cellular secretion

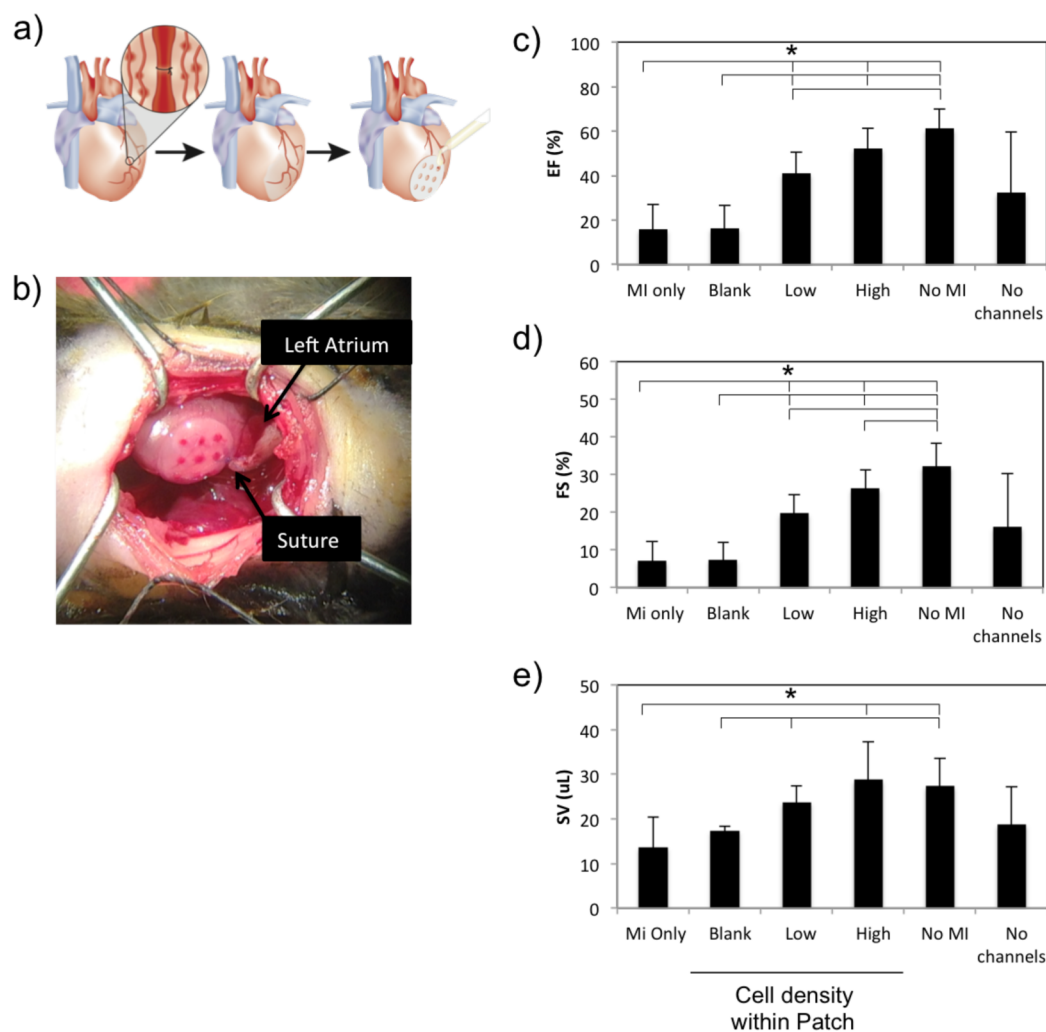


Figure 4. Evaluation of the gel patch to recovering cardiac function of hearts injured by vascular occlusion. (a) Schematic representation of the in vivo murine myocardial infarction studies depicts the occlusion of the left coronary artery, the blanching of the left ventricular wall that accompanies the occlusion, and the placement of the patch and subsequent addition of the fibrin based glue to ensure patch adherence. (b) Supplementing the schematic representation is a live-image of the final placement of the construct on the epicardial surface of the heart. (c–e) Echocardiogram measurements of (c) ejection fraction (EF), (d) fractional shortening (FS), and (e) stroke volume (SV) show comparative assessments of cardiac function among mice receiving no treatment (MI only), those implanted with blank gel patch (Blank), those implanted with the microchanneled gel patch laden with MSCs at densities of 0.4×10^6 cells/mL (low) and 2.0×10^6 cells/mL (high), those without MI (No MI), and those implanted with the microchannel-free gel patch laden with MSCs at a density of 2.0×10^6 cells/mL (no channels). The microchannel diameter was kept constant at $500 \mu\text{m}$. Asterisks (*) represent statistical significance of the difference of the values between conditions ($p < 0.05$).

of VEGF level, in particular for the higher cell density at 2.0×10^6 cells/mL. The significant decrease of the cellular VEGF secretion level for the cells loaded into the $1000 \mu\text{m}$ -diameter microchanneled gels is attributed to the decreased cell number because of active cell migration outward the gel.

Therapeutic Activity of the MSC-Laden Gel Patch Using the Mouse MI model. A mouse MI model was used to test the efficacy of the MSC-laden hydrogel patch to alleviating the remodeling of the heart following ischemic injury. The left coronary artery was occluded to mimic the blockage of blood flow to the left ventricle that is characteristic of the majority of MI (Figure 4a). A blanching of the myocardium downstream of the occluded vessel could be seen almost instantaneously, confirming the identification of the ischemic tissue. Echocardiogram measurements were then performed to analyze the heart function with and without gel patches. The LAD occlusion resulted in a significant reduction in the ejection fraction (EF) (from $61 \pm 9\%$ to $16 \pm 11\%$), fractional shortening (FS) (from 31

$\pm 6\%$ to $7 \pm 5\%$), and stroke volume (SV) (from $28 \pm 6\%$ to $14 \pm 7\%$).

Immediately following the occlusion, the gel patch was placed directly on the ischemic tissue (Figure 4a, b). A fibrin-based glue was applied to the exterior of the patch to ensure adherence of the gel to the myocardium. On the basis of the in vitro experiments, the MSC-laden hydrogel patch with $500 \mu\text{m}$ -diameter microchannels and MSC-laden gel patch without microchannels were used for therapies. The MSC-laden hydrogel patch with $1000 \mu\text{m}$ -diameter microchannels was excluded because of small difference of the cytokine secretion profile from the patch with $500 \mu\text{m}$ -diameter microchannels.

Echocardiograph measurements taken 5 weeks postoperatively showed a significant increase of EF and SV in the hearts treated with the MSC-laden patch with microchannels (Figure 4c–e). Although not statistically significant, a stepwise improvement was noticed with an increase in cell density. In particular, microchanneled gel patches loaded with MSCs at a

density of 2.0×10^6 cells/mL led to the EF and SV levels similar to those of mice that were not subject to MI. Patches containing no cells (marked with “blank” in Figure 4c–e) led to limited recovery of cardiac function, similar to the untreated group (marked with “MI only”). More interestingly, the MSC-laden gel patch without microchannels (marked with “No channels” in Figure 4c–e) displayed a sporadically lower recovery level of cardiac function.

Animals were sacrificed at 8 weeks after the surgery. Histological analysis showed a clear collagen deposition in the untreated mice (marked with “MI only”), a characteristic of cardiomyocytes necrosis and scar tissue formation (Figure 5a). Left ventricular dilation and wall thinning were also seen in the “MI only” condition, and mice implanted with a cell-free

microchanneled gel patch (marked with “Blank”). The microchanneled gel patches with MSCs at a density of 0.4×10^6 cells/mL (marked with “Low density patch”) displayed a slight decrease in cardiac fibrosis and left ventricular dilation. Finally, mice treated with microchanneled gel patches laden with MSCs at a density of 2.0×10^6 cells/mL (marked with “High density patch”) showed very little necrosis at the site of injury, with little to no ventricular dilation and wall thinning. The left ventricular and septal thicknesses quantified with the histological images were further normalized to the ventricular diameter. These quantifications confirmed that the MSC-laden gel patches increased the normalized left ventricular and septal thickness compared to the negative controls (Figure 5b, c). In a previously published study, we demonstrated the lack of damage to the surrounding myocardial tissue 7 days after placement of a control patch on noninfarcted tissue.³¹

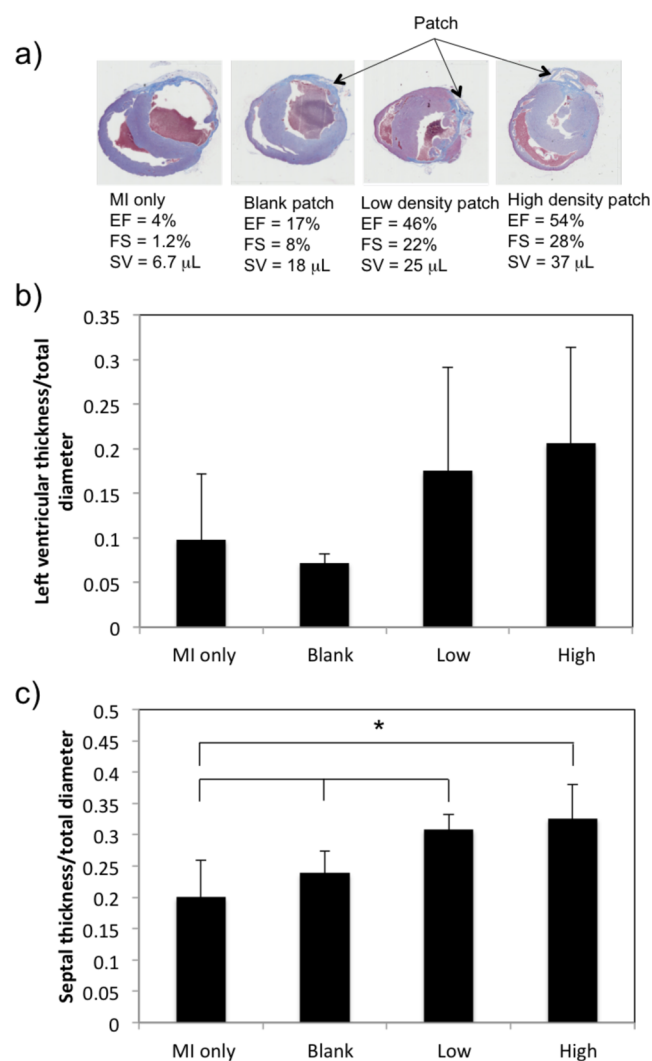


Figure 5. Histological analysis. (a) Representative 8 week histological images of each condition are shown along with their respective functional measurements. The constructs can clearly be seen, and a decrease in fibrosis and collagen deposition (blue staining) can be appreciated with implantation of the MSC-laden, microchanneled hydrogel patch. Quantitative analysis of (b) left ventricular free wall thickness and (c) septal thickness normalized to the overall heart diameter show an increase in each with implantation of the MSC-laden, microchanneled hydrogel patch. Asterisks (*) represent statistical significance of the difference of the values between conditions ($p < 0.05$).

DISCUSSION

This study demonstrated that the 3D printed PEGDMA hydrogel patch with microchannels of controlled diameters could encapsulate MSCs without affecting cellular ability to secrete therapeutic cytokines and subsequently enhance therapeutic quality to treat cardiac muscle damaged by MI. Using the SLA, the MSC-laden gel patch was assembled to present microchannels with diameters appropriate for sustained release of multiple therapeutic cytokines from cells and subsequent diffusion of the cytokines into target tissue, while minimizing cell loss. The MSC-laden microchanneled gel implanted on heart damaged by coronary artery occlusion showed enhanced recovery of cardiac function and minimizing cardiac remodeling, compared with multiple control conditions.

This study strengthens the importance of paracrine factors to aid in the prevention of myocardial damage post-MI. We have previously calculated the pore diameter of our gel constructs to be approximately 11 nm, large enough to allow cytokine secretion while still maintaining cells encapsulated within the construct. Further studies in the field have reported that the cardioprotective effect of MSCs lies not only in their secretion of individual cytokines, but also in the secretion of larger exosomes.³³ Based on the pore size of the PEDGMA hydrogel, our current platform, which remains stable in physiological conditions, may not be able to release these particles. Further modification of the gel to expand or degrade in a physiological condition may enable us to attain a therapeutic synergy by delivering both biomolecules and exosomes.

In a previous study, we established that 500 μm -diameter microchannels 3D printed in a hydrogel enhanced localization of cell-secreting factors and more effectively stimulated cytokine release from host cells than constructs without microchannels.³² This result implicated that therapeutic outcomes are dependent more on the concentrated flux of cytokines into the microchannels than the total amount of cytokine released. In particular, compared with the microchannel-free gel patch, this microchanneled gel patch allowed for greater and directed angiogenic potential at the site of the microchannels, resulting in a more beneficial outcome. We propose that further decrease of microchannel diameter to 200 to 300 μm would increase the amount of cell-secreting factors into implanted tissue. This smaller-diameter microchannels can be incorporated into the gel constructs using a microSLA we recently assembled to fabricate a 3D gel construct with a higher resolution.³⁴

In this paper, we have demonstrated the cessation of cardiac remodeling following myocardial infarction, resulting in the prevention of tissue necrosis and scar tissue formation. Although tissue fibrosis has always thought to be a terminal process, studies on liver cirrhosis have demonstrated its reversibility with subsequent cell regeneration.^{35–38} Translation of these findings to the myocardium, our cardiac patch could be utilized for the reversal of damage caused by vascular insult. By this method, treatment success would be independent of the time elapsed between injury to intervention. Although we have yet to explore this possibility, we intend to explore fibrotic reversal as a promising avenue for future directions in the field.

In a similar context, this study demonstrated that microchannel architecture was an important factor to prevent injury of cardiac muscle damaged by MI. The MSC-laden gel patch without microchannels resulted in a decrease in reproducibility of cardiac protection, as was seen in the large statistical variation of outcomes. In contrast, the microchanneled gel patch could improve cardiac function in a reproducible manner, while minimizing terminal scar formation. More interestingly, the therapeutic function of the gel patch was not significantly dependent on the cell density, thus enabling us to propose that the microchanneled gel patch is advantageous to reducing the number of required cells for therapies. This feature would greatly help alleviating the translational burden of collecting and culturing MSCs for clinical use.

CONCLUSIONS

In conclusion, this 3D printed, microchanneled hydrogel laden with MSCs would become an advanced therapeutic tool that can sustainably deliver multiple therapeutics to the site of injury and improve therapeutic quality of ischemic heart injury. We propose that the microchannels in the gel play an important role in releasing cell-secreting therapeutic cytokines into target tissue by removing gel–tissue interface, a physical barrier for biomolecular transports. This study provides a promising cell-based drug delivery system that aids the prevention of detrimental tissue remodeling following acute injury.

AUTHOR INFORMATION

Corresponding Author

*E-mail: hjkong06@illinois.edu.

Notes

The authors declare no competing financial interest.

ACKNOWLEDGMENTS

This work was supported by National Science Foundation (CBET-140349 & STC-EBICS Grant CBET-0939511 to H.K.), Telemedicine and Advanced Technology Research Center (W81XWH-08-1-0701), a fellowship from Carle Foundation Hospital, and partially National Institutes of Health (1R01 HL109192 to H.K.).

REFERENCES

(1) Anderson, J. L.; Adams, C. D.; Antman, E. M.; Bridges, C. R.; Califf, R. M.; Casey, D. E.; Chavey, W. E.; Fesmire, F. M.; Hochman, J. S.; Levin, T. N.; et al. ACC/AHA 2007 guidelines for the management of patients with unstable angina/non-ST-Elevation myocardial infarction: a report of the American College of Cardiology/American Heart Association Task Force on Practice Guidelines (Writing Committee to Revise the 2002 Guidelines for the Management of Patients With Unstable Angina/Non-ST-Elevation Myocardial Infarction) developed in collaboration with the American College of

Emergency Physicians, the Society for Cardiovascular Angiography and Interventions, and the Society of Thoracic Surgeons endorsed by the American Association of Cardiovascular and Pulmonary Rehabilitation and the Society for Academic Emergency Medicine. *J. Am. Coll. Cardiol.* **2007**, *50* (7), e1–e157.

(2) Gibbons, R. J.; Holmes, D. R.; Reeder, G. S.; Bailey, K. R.; Hopfenspirger, M. R.; Gersh, B. J. Immediate angioplasty compared with the administration of a thrombolytic agent followed by conservative treatment for myocardial infarction. The Mayo Coronary Care Unit and Catheterization Laboratory Groups. *N. Engl. J. Med.* **1993**, *328* (10), 685–691.

(3) Killip, T.; Kimball, J. T. Treatment of myocardial infarction in a coronary care unit. *Am. J. Cardiol.* **1967**, *20* (4), 457–464.

(4) Mello, B. H. G. de; Oliveira, G. B. F.; Ramos, R. F.; Lopes, B. B. C.; Barros, C. B. S.; Carvalho, E. de O.; Teixeira, F. B. P.; Arruda, G. D. S.; Revelo, M. S. C.; Piegas, L. S. Validation of the Killip-Kimball Classification and Late Mortality after Acute Myocardial Infarction. *Arq. Bras. Cardiol.* **2014**, DOI: [10.5935/abc.20140091](https://doi.org/10.5935/abc.20140091).

(5) Gottlieb, R. A.; Burleson, K. O.; Kloner, R. A.; Babior, B. M.; Engler, R. L. Reperfusion injury induces apoptosis in rabbit cardiomyocytes. *J. Clin. Invest.* **1994**, *94* (4), 1621–1628.

(6) Bolli, R. Oxygen-derived free radicals and myocardial reperfusion injury: an overview. *Cardiovasc. Drugs Ther.* **1991**, *5* (Suppl 2), 249–268.

(7) Wollert, K. C. Mesenchymal Stem Cells for Myocardial Infarction: Promises and Pitfalls. *Circulation* **2005**, *112* (2), 151–153.

(8) Shake, J. G.; Gruber, P. J.; Baumgartner, W. A.; Senechal, G.; Meyers, J.; Redmond, J. M.; Pittenger, M. F.; Martin, B. J. Mesenchymal stem cell implantation in a swine myocardial infarct model: engraftment and functional effects. *Ann. Thorac. Surg.* **2002**, *73* (6), 1919–1925.

(9) Price, M. J.; Chou, C.-C.; Frantzen, M.; Miyamoto, T.; Kar, S.; Lee, S.; Shah, P. K.; Martin, B. J.; Lill, M.; Forrester, J. S.; et al. Intravenous mesenchymal stem cell therapy early after reperfused acute myocardial infarction improves left ventricular function and alters electrophysiologic properties. *Int. J. Cardiol.* **2006**, *111* (2), 231–239.

(10) Dai, W.; Hale, S. L.; Martin, B. J.; Kuang, J.-Q.; Dow, J. S.; Wold, L. E.; Kloner, R. A. Allogeneic mesenchymal stem cell transplantation in postinfarcted rat myocardium: short- and long-term effects. *Circulation* **2005**, *112* (2), 214–223.

(11) Pittenger, M. F.; Martin, B. J. Mesenchymal stem cells and their potential as cardiac therapeutics. *Circ. Res.* **2004**, *95* (1), 9–20.

(12) Gnecci, M. Evidence supporting paracrine hypothesis for Akt-modified mesenchymal stem cell-mediated cardiac protection and functional improvement. *FASEB J.* **2006**, *20* (6), 661–669.

(13) Zimmermann, J. A.; Mcdevitt, T. C. Pre-conditioning mesenchymal stromal cell spheroids for immunomodulatory paracrine factor secretion. *Cytotherapy* **2014**, *16* (3), 331–345.

(14) Ylostalo, J. H.; Bartosh, T. J.; Tiblow, A.; Prockop, D. J. Unique characteristics of human mesenchymal stromal/progenitor cells pre-activated in 3-dimensional cultures under different conditions. *Cytotherapy* **2014**, *16* (11), 1486–1500.

(15) Huang, B.; Qian, J.; Ma, J.; Huang, Z.; Shen, Y.; Chen, X.; Sun, A.; Ge, J.; Chen, H. Myocardial transfection of hypoxia-inducible factor-1 α and co-transplantation of mesenchymal stem cells enhance cardiac repair in rats with experimental myocardial infarction. *Stem Cell Res. Ther.* **2014**, *5* (1), 22.

(16) Berry, M. F.; Engler, A. J.; Woo, Y. J.; Pirolli, T. J.; Bish, L. T.; Jayasankar, V.; Morine, K. J.; Gardner, T. J.; Discher, D. E.; Sweeney, H. L. Mesenchymal stem cell injection after myocardial infarction improves myocardial compliance. *Am. J. Physiol. Heart Circ. Physiol.* **2006**, *290* (6), H2196–2203.

(17) Iso, Y.; Spees, J. L.; Serrano, C.; Bakondi, B.; Pochampally, R.; Song, Y.-H.; Sobel, B. E.; Delafontaine, P.; Prockop, D. J. Multipotent human stromal cells improve cardiac function after myocardial infarction in mice without long-term engraftment. *Biochem. Biophys. Res. Commun.* **2007**, *354* (3), 700–706.

- (18) Ohnishi, S.; Yanagawa, B.; Tanaka, K.; Miyahara, Y.; Obata, H.; Kataoka, M.; Kodama, M.; Ishibashi-Ueda, H.; Kangawa, K.; Kitamura, S.; et al. Transplantation of mesenchymal stem cells attenuates myocardial injury and dysfunction in a rat model of acute myocarditis. *J. Mol. Cell. Cardiol.* **2007**, *42* (1), 88–97.
- (19) Li, Y.; Sheng, Z.; Yang, Y.; Yao, Y.; Ma, G. Dual-modal tracking of transplanted mesenchymal stem cells after myocardial infarction. *Int. J. Nanomed.* **2011**, *815*.
- (20) Jin, J.; Jeong, S. I.; Shin, Y. M.; Lim, K. S.; Shin, H. S.; Lee, Y. M.; Koh, H. C.; Kim, K.-S. Transplantation of mesenchymal stem cells within a poly(lactide-*co*- ϵ -caprolactone) scaffold improves cardiac function in a rat myocardial infarction model. *Eur. J. Heart Failure* **2009**, *11* (2), 147–153.
- (21) Levit, R. D.; Landazuri, N.; Phelps, E. A.; Brown, M. E.; Garcia, A. J.; Davis, M. E.; Joseph, G.; Long, R.; Safley, S. A.; Suever, J. D.; et al. Cellular Encapsulation Enhances Cardiac Repair. *J. Am. Heart Assoc.* **2013**, *2* (5), e000367–e000367.
- (22) Ryu, J.; Kim, I.; Cho, S.; Cho, M.; Hwang, K.; Piao, H.; Piao, S.; Lim, S.; Hong, Y.; Choi, C. Implantation of bone marrow mononuclear cells using injectable fibrin matrix enhances neovascularization in infarcted myocardium. *Biomaterials* **2005**, *26* (3), 319–326.
- (23) Piao, H.; Kwon, J.-S.; Piao, S.; Sohn, J.-H.; Lee, Y.-S.; Bae, J.-W.; Hwang, K.-K.; Kim, D.-W.; Jeon, O.; Kim, B.-S.; et al. Effects of cardiac patches engineered with bone marrow-derived mononuclear cells and PGCL scaffolds in a rat myocardial infarction model. *Biomaterials* **2007**, *28* (4), 641–649.
- (24) Uemura, R.; Xu, M.; Ahmad, N.; Ashraf, M. Bone marrow stem cells prevent left ventricular remodeling of ischemic heart through paracrine signaling. *Circ. Res.* **2006**, *98* (11), 1414–1421.
- (25) Heidemann, J. Angiogenic Effects of Interleukin 8 (CXCL8) in Human Intestinal Microvascular Endothelial Cells Are Mediated by CXCR2. *J. Biol. Chem.* **2003**, *278* (10), 8508–8515.
- (26) Chu, H.; Wang, Y. Therapeutic angiogenesis: controlled delivery of angiogenic factors. *Ther. Delivery* **2012**, *3* (6), 693–714.
- (27) Frangogiannis, N. G. Critical Role of Endogenous Thrombospondin-1 in Preventing Expansion of Healing Myocardial Infarcts. *Circulation* **2005**, *111* (22), 2935–2942.
- (28) Kinnaird, T.; Stabile, E.; Burnett, M. S.; Lee, C. W.; Barr, S.; Fuchs, S.; Epstein, S. E. Marrow-derived stromal cells express genes encoding a broad spectrum of arteriogenic cytokines and promote in vitro and in vivo arteriogenesis through paracrine mechanisms. *Circ. Res.* **2004**, *94* (5), 678–685.
- (29) Mirotsov, M.; Jayawardena, T. M.; Schmeckpeper, J.; Gnechi, M.; Dzau, V. J. Paracrine mechanisms of stem cell reparative and regenerative actions in the heart. *J. Mol. Cell. Cardiol.* **2011**, *50* (2), 280–289.
- (30) Chan, V.; Zorlutuna, P.; Jeong, J. H.; Kong, H.; Bashir, R. Three-dimensional photopatterning of hydrogels using stereolithography for long-term cell encapsulation. *Lab Chip* **2010**, *10* (16), 2062–2070.
- (31) Melhem, M.; Jensen, T.; Reinkensmeyer, L.; Knapp, L.; Flewellyn, J.; Schook, L. A Hydrogel Construct and Fibrin-based Glue Approach to Deliver Therapeutics in a Murine Myocardial Infarction Model. *J. Visualized Exp.* **2015**, No. 100, e52562.
- (32) Jeong, J. H.; Chan, V.; Cha, C.; Zorlutuna, P.; Dyck, C.; Hsia, K. J.; Bashir, R.; Kong, H. A “Living” Microvascular Stamp: “Living” Microvascular Stamp for Patterning of Functional Neovessels; Orchestrated Control of Matrix Property and Geometry (Adv. Mater. 1/2012). *Adv. Mater.* **2012**, *24* (1), 1–1.
- (33) Lai, R. C.; Arslan, F.; Lee, M. M.; Sze, N. S. K.; Choo, A.; Chen, T. S.; Salto-Tellez, M.; Timmers, L.; Lee, C. N.; El Oakley, R. M.; et al. Exosome secreted by MSC reduces myocardial ischemia/reperfusion injury. *Stem Cell Res.* **2010**, *4* (3), 214–222.
- (34) Raman, R.; Bhaduri, B.; Mir, M.; Shkumatov, A.; Lee, M. K.; Popescu, G.; Kong, H.; Bashir, R. Bioprinting: High-Resolution Projection Microstereolithography for Patterning of Neovasculature (Adv. Healthcare Mater. 5/2016). *Adv. Healthcare Mater.* **2016**, *5* (5), 622–622.
- (35) Kisseleva, T.; Cong, M.; Paik, Y.; Scholten, D.; Jiang, C.; Benner, C.; Iwaisako, K.; Moore-Morris, T.; Scott, B.; Tsukamoto, H.; et al. Myofibroblasts revert to an inactive phenotype during regression of liver fibrosis. *Proc. Natl. Acad. Sci. U. S. A.* **2012**, *109* (24), 9448–9453.
- (36) Friedman, S. L.; Sheppard, D.; Duffield, J. S.; Violette, S. Therapy for fibrotic diseases: nearing the starting line. *Sci. Transl. Med.* **2013**, *5* (167), 167sr1.
- (37) Marcellin, P.; Gane, E.; Buti, M.; Afdhal, N.; Sievert, W.; Jacobson, I. M.; Washington, M. K.; Germanidis, G.; Flaherty, J. F.; Aguilar Schall, R.; et al. Regression of cirrhosis during treatment with tenofovir disoproxil fumarate for chronic hepatitis B: a 5-year open-label follow-up study. *Lancet* **2013**, *381* (9865), 468–475.
- (38) D’Ambrosio, R.; Aghemo, A.; Rumi, M. G.; Ronchi, G.; Donato, M. F.; Paradis, V.; Colombo, M.; Bedossa, P. A morphometric and immunohistochemical study to assess the benefit of a sustained virological response in hepatitis C virus patients with cirrhosis. *Hepatology* **2012**, *56* (2), 532–543.